LIMNOLOGY
and
OCEANOGRAPHY: METHODS

Limnol. Oceanogr.: Methods 8, 2010, 241–253

A comparative study of methods for surface area and three-dimensional shape measurement of coral skeletons

C. J. Veal[1], G. Holmes[1], M. Nunez[2], O. Hoegh-Guldberg[1], and J. Osborn[2]*
[1]Global Climate Institute, The University of Queensland, St Lucia, Queensland, Australia, 4072
[2]School of Geography and Environmental Studies, University of Tasmania, Hobart, Tasmania, Australia, 7001

Abstract

The three-dimensional morphology and surface area of organisms such as reef-building corals is central to their biology. Consequently, being able to detect and measure this aspect of corals is critical to understanding their interactions with the surrounding environment. This study explores six different methods of three-dimensional shape and surface area measurements using the range of morphology associated with the Scleractinian corals: *Goniopora tenuidens, Acropora intermedia*, and *Porites cylindrica*. Wax dipping; foil wrapping; multi-station convergent photogrammetry that used the naturally occurring optical texture for conjugate point matching; stereo photogrammetry that used projected light to provide optical texture; a handheld laser scanner that employed two cameras and a structured light source; and X-ray computer tomography (CT) scanning were applied to each coral skeleton to determine the spatial resolution of surface detection as well as the accuracy of surface area estimate of each method. Compared with X-ray CT, wax dipping provided the best estimate of the surface area of coral skeletons that had external corallites, regardless of morphological complexity. Foil wrapping consistently showed a large degree of error on all coral morphologies. The photogrammetry and laser-scanning solutions were effective only on corals with simple morphologies. The two techniques that used projected lighting were both subject to skeletal light scattering, caused by both gross morphology and meso-coral architecture and which degraded signal triangulation, but otherwise provided solutions with good spatial resolution. X-ray CT scanning provided the highest resolution surface area estimates, detecting surface features smaller than 1000 μm^2.

The surface area of biological organisms is a fundamental parameter that is critical to understanding their interaction with external physical and biological processes (Bythell et al. 2001). In the case of habitat-forming marine organisms such as Scleractinian corals, surface area plays a critical role in determining photosynthetic and calcification rates, nutrient exchange, and visible and ultraviolet irradiance exposure (Helmuth et al. 1997; Hoegh-Guldberg and Williamson 1999; Lesser et al. 2000), which ultimately dictate the construction of complex three dimensional (3-D) structures into which more than a million coral reef species are found (Hoegh-Guldberg 1999; Yentsch et al. 2002; Hughes et al. 2003).

Optical systems for mapping surface topography are often classified as either passive or active. Passive systems are those for which the mathematical solution does not rely on a projected or emitted signal with known metric geometry. Passive systems include traditional multi-image photogrammetry, as well as methods to derive shape from shading, silhouette, edges, or from measures of focus/defocus (Remondino and El-Hakim 2006; Wöhler 2009). Passive photogrammetric techniques generally rely on ambient illumination of an object and include solutions derived from measuring conjugate points appearing in two photographic images (in either a normal-case stereo or a convergent camera geometry); or measuring conjugate points in multiple photographic images (three or more

*Corresponding author: E-mail: c.veal@uq.edu.au

Acknowledgments

The authors would like to acknowledge assistance from Mr. Rob Anders at the Centre for Spatial Information Science, University of Tasmania, for use of the optical texture scanner. Laser scanning was made possible through the assistance of Dr. Jim Hanan, Centre for Excellence for Integrative Legume Research, The University of Queensland. X-ray CT scanning was facilitated with the assistance of Mrs. Morag Wilson at the School of Veterinary Science, The University of Queensland. This manuscript has benefited from the comments and suggestions of two anonymous reviewers. This research was partly funded by the Australian Research Council Centre for Excellence for Coral Reef Studies (to OHG), an International Society for Optical Engineering, 2007 SPIE Student Bursary Program (to CV), and Australian Research Council industry linkage with the United States of America's National Oceanic and Atmospheric Administration.

DOI 10.4319/lom.2010.8.241

images, again in either normal-case stereo configurations or using convergent geometries). Photogrammetric techniques rely on the object surface having sufficient natural or artificial targets, or sufficient optical texture, to allow conjugate points to be matched across two or more images. In some cases, this optical texture can be achieved by projecting a pattern onto the surface of the object at the moment of image capture. The pattern provides optical texture only; the geometry of the projection is neither known nor required in the solution.

Active systems for mapping surface topography are those that employ a projected or emitted signal and where the geometry or some other property (such as a modulated wavelength) of that signal is known (metric) and is integral to the computation of shape (Beraldin 2004). Active systems include structured light triangulation, in which a single spot, sheet of light, or bundle of rays is projected, and where the geometry of that projection is known and employed in the solution. Structured light triangulation methods include, for example, systems that employ one metric pattern projector and one metric camera, with 3-D location derived from the triangulation of the projected and imaged light. Active systems also include time delay methods, where the solution relies on knowing the direction and propagation parameters (wavelength, velocity, time of flight) of an emitted signal. Remondino and El-Hakim (2006) provide a useful classification and review of noncontact systems for object measurement. In Table 1, their classification has been modified to provide more details of the photogrammetric solutions. *See* also Atkinson (1996), Luhmann et al. (2006), and Fryer et al. (2007) for useful summaries of noncontact close-range measurement systems and techniques.

A multitude of methods have been tested in the last 60 years to measure the surface area and shape of corals (Table 2). The direct measurement of coral tissue surface area is logistically challenging, with only a few studies that used X-ray medical imaging equipment succeeding (Laforsch et al. 2008; Naumann et al. 2009). The majority of methods for surface area measurement on coral skeletons are based on the estimation of the "primary" surface area, as defined in Hoegh-Guldberg (1988), which includes the surface area of coral tissue and polyps. In most Scleractinian corals, the layer of coral tissue above the skeleton is very small, therefore allowing the coral

Table 1. Three-dimensional acquisition systems for object measurement using noncontact methods, adapted from Remondino and El-Hakim (2006).

Passive systems	Photogrammetry	These methods include two image (stereo) photogrammetry, or multi-image, convergent, photogrammetry. The solution may employ (nonmetric) light projection to ensure that object surfaces have sufficient optical texture to allow for matching of conjugate points appearing in two or more photographic images, or may rely on the inherent optical texture of the object or surface.
	Shape from	Shading, silhouette, edges, texture, focus/defocus.
Active systems	Structured light triangulation	These methods employ (metric) projection of a single spot, sheet of light, or bundle of rays that is imaged by a metric camera.
	Time delay	These methods employ time of flight measurement and include pulse- and phase-based LiDAR and interferometric techniques.

Table 2. List of different methods, with authors, used to extract surface area and shape information from coral skeletons, categorized by their ability to work on massive (M), simple branching (SB), and complex branching structures (CB), as well as their success with yielding information about the gross morphology (GM) and meso-scale architecture of the corals, and the time taken to collect and extract that information.

Method	M	SB	CB	GM	Meso	Time	Author(s)
Aluminium foil	Yes	Yes	Limit	Yes	No	10 min	Marsh (1970)
Paraffin wax	Yes	Yes	Yes	Yes	No	10 min	Stimson and Kinzie (1991)
Latex	Yes	Yes	Yes	Yes	No	10 min	Meyers and Schultz (1985)
Dye	Yes	Yes	Yes	Yes	No	10 min	Hoegh-Guldberg (1988)
Surface index	Yes	No	No	Limit	No	N/A	Dahl (1973); Chancerelle (2000); Holmes (2008)
Geometric shape fitting	Yes	Yes	No	Yes	No	10 min	Odum and Odum 1955; Jones et al. (2008)
Stereo photogrammetry	Yes	Limit	No	Limit	No	1 h	Done (1981)
Stereo video	Yes	Limit	No	Yes	No	3-4 h	Cocito et al. (2003)
Photogrammetric reconstruction	Yes	Limit	No	Yes	No	3-4 h	Bythell et al. (2001)
Laser scanning	Yes	Yes	Limit	Yes	No	2-3 h	Holmes (2008); Raz-Bahat et al. (2009)
Structured light	Yes	Yes	Limit	Yes	Yes	3-4 h	This article
X-Ray CT	Yes	Yes	Yes	Yes	Yes	1-2 h	Laforsch et al. (2008); Naumann et al. (2009)

skeleton to be used as suitable proxy of the coral tissue surface area (Laforsch et al. 2008). Early methods involved the use of surface area indexes, where representative geometric surfaces were used to approximate the actual coral surface and a mathematical expression used to estimate surface area (Odum and Odum 1955; Dahl 1973). Whereas these methods were advantageous, as they were nondestructive, the surface area approximations of single colonies were poorly represented for many common coral growth forms (Laforsch et al. 2008). Other methods such as wrapping in foil (Marsh 1970), dipping in wax or latex (Meyers and Shultz 1985; Stimson and Kinzie 1991), or the use of varnish and immersion in dye (Hoegh-Guldberg 1988) were generally destructive. In each case, the mass of the measuring material or its displacement volume were related to surface area using a calibration curve. These methods, though effective at giving an estimate of the surface area of the coral skeleton, generally underestimate the surface area by failing to detect corallite meso-architecture and are limited by both the destructive nature of data collection and the size of the corals that can be measured (Hoegh-Guldberg 1988; Bythell et al. 2001; Cocito et al. 2003).

The bulk of the literature on nondestructive methods for surface area extraction from corals employs passive systems. Single-image reconstruction based on volumetric equations has been used to determine the surface area of *Millepora dichotoma* in the Red Sea and proved reliable for this coral that is characterized by flat plates with holes in between the braches (Ben-Zion et al. 1991). Reconstructions of single, simple branches of corals commonly used in experimental coral research has also been achieved using manual alignment of digital spline curves onto the coral in a sequence of orthogonal photographs, facilitating a nondestructive method of surface area extraction of live tissue samples (Jones et al. 2008). Done (1981) used stereo photogrammetry for survey work in the Great Barrier Reef, where it was shown to be a time-efficient method for determining the surface area of different coral species. The revolution of aquatic photogrammetry for 3-D surface areas came with the production and use of commercially available software programs for the digitization and reconstruction of multiple photos into 3-D shapes. Bythell et al. (2001) were the first to experiment with multiple convergent photographs and digital photogrammetry software (Photomodeler, EOS Systems), reconstructing the surface area of foam test objects and then field validating the application on hemispherical corals in the US Virgin Islands. This work was then extended by Courtney et al. (2007) using a more recent version of Photomodeler in conjunction with Rhinoceros® (McNeel) NURBS modeling for higher resolution reconstruction of the coral surface. These various passive photographic methods indicate the significant possibilities of nondestructive, in situ photogrammetric shape capture, but have been limited to modeling hemispherical and simple branching corals. Whereas these may represent the Caribbean Reefs well (Jones et al. 2008; Cocito et al. 2003), for most other regions of the world, where coral reefs are dominated by more complex branching morphologies, their application is limited (Bythell et al. 2001; Cocito et al. 2003; Courtney et al. 2007).

Active shape capture systems commonly use optical triangulation, where the 3-D location of any one point on the object is calculated by computing the intersection of two lines in three-dimensional space. One of these lines is projected by the active sensor creating, for example, a small, well-defined, unambiguous laser dot on the object, and the other line is defined by the light reflected from that dot and passing through the lens of a calibrated camera (Remondino and El-Hakem 2006). In these systems, the geometry of the light emitter and of the camera is accurately known (calibrated). The primary limitation of passive or active measurement systems that rely on triangulation is that a single point on the object surface must be visible from at least two or more sensor locations in order for the triangulation to be computed. This is necessarily restrictive when dealing with structurally complex objects, such as branching or foliaceous corals. The accuracy of any method that relies on reflected light, particularly strong light, for object targeting also depends in-part upon the surface properties of the object being scanned (Beraldin et al. 2005). An "ideal surface" for shape capture is defined as being opaque, with Lambertian reflection and surface homogeneity (Beraldin et al. 2005). For most surfaces, including corals, this is not the case. Many surfaces are optically transparent to active scanner emission sources, with nonuniform surface light reflection and internal light scattering within the meso-architecture of coral polyps (Barnes and Devereux 1988; Enriquez et al. 2005). Accurate surface reconstructions and surface area estimates can only be achieved if an appropriate standard method is used where the sources of error are known and controlled (Remondino and El-Hakim 2006).

An alternative method of active shape capture, widely used for shape-capture of objects of variable density and surface complexity, and that can be used for calcareous corals is X-ray computer tomography (CT) (Kruszynski et al. 2007). In the case of X-ray CT scanning, the emission source is a horizontal fan-shaped X-ray beam that penetrates the object and is collected on a series of scintillators on the other side (Ketcham and Carlson 2001). X-ray attenuation by coral skeletons is a function of the ratio of solid skeleton to internal corallite structure, seasonal aragonite deposition levels, and the quantum energy of the incident X-Rays (Le Tissier et al. 1994). Each consecutive X-ray slice is compiled using medical imaging software to create a 3-D image. The significant difference between X-ray CT and other active projection shape capture methods is that both the surface and subsurface structures are recorded (Kruszynski et al. 2007). X-ray CT represents the most spatially accurate method of shape capture of corals currently available, making its use as a standard to apply to other methods highly desirable (Laforsch et al. 2008; Naumann et al. 2009).

The increased use of various published methods for the capture of shape and surface area information from coral

skeletons necessitates comparison between each method, especially in terms of their advantages and limitations within particular study settings. This study compares six methods that are capable of capturing the surface areas and shape of coral skeletons, namely: wax dipping; foil wrapping; two passive photogrammetric approaches; one active laser-scanning approach that employs optical triangulation; and X-ray CT scanning. In addition, this article investigates the scattering and accuracy of systems that employ projected light on coral skeletons, as well as contrasting differing spatial resolution, processing time, and cost-effective methods to generate 3-D models of coral skeletons.

Materials and procedures

Coral samples—This study used three taxonomically and morphologically different Scleractinian coral skeletons *Goniopora tenuidens* (Quelch 1886), *Acropora intermedia* (Brook 1891) and *Porites cylindrica* (Dana 1846) based on their gross morphological and meso-architectural complexity. The coral skeletons (Fig. 1) were obtained from The University of Queensland coral skeleton collection and were cleaned using a dilute sodium hypochlorite solution to remove any residual tissue before being rinsed, air dried, and mounted on reference tiles with molding putty.

Optical transparency testing—Skeletal scattering was assessed with two emission sources, a 1-mW red laser (630 nm) and a LCD projector. The laser was connected to a regulated 240 V mains powered, 3 V DC power source, to maintain output consistency throughout the experiment and checked periodically with a LiCor LI-189 PAR (LI-COR Biosciences) radiometer, mounted at the end of a blackened 100 mm tube. The Hitachi CP-X345 (Hitachi) white light projector used as the projection source for the optical texture scanner was programmed to produce a single spot 30 mm in diameter, 0.6 m distance from the target. This spot size was selected to mimic both the laser spot size and the normal projected dot size used during optical texture scanning. Light scattering was assessed by mounting the light source below a tripod mounted Canon Powershot 630 (Canon) 8.0 megapixel camera, calibrated at its full optical focal length of 29.2 cm. Photographs were taken in a dark room, with a shutter speed of 1/100 and F stop of 4. The light sources were offset at < 2° to reduce any effects of non-Lambertian surface properties of the coral skeletons or calibration tiles. A calcium carbonate tile that was spray painted several times with matte black paint (White Knight) was used as a calibration surface to determine the number of pixels occupied by the emission source in the camera frame without scattering. Thirty photographs of each skeleton were taken at 3° horizontally rotated increments using a mechanical grade rotating stage. In addition to the three coral skeletons outlined above, samples of *A. intermedia* collected from the same parent colony were broken into smaller pieces and treated with white and black matte spray paint (White Knight) to test the effectiveness of surface treatments to reduce skeletal scattering. Photographs

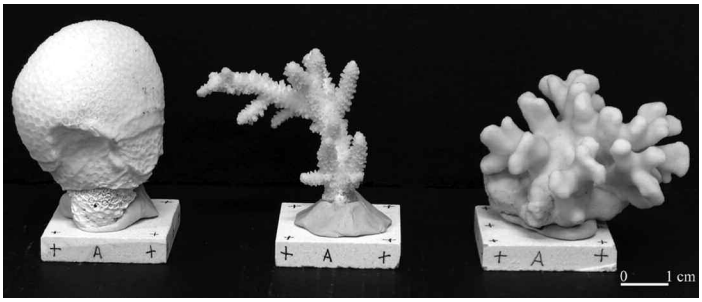

Fig. 1. Photograph of the 3 coral skeletons, (L-R) *Goniopora tenuidens*, *Acropora intermedia*, and *Porites cylindrica*, used in this study. Each coral skeleton was selected for its gross morphology and meso-architecture, with the *G. tenuidens* comprising gross morphology, with internal corallite structure; *A. intermedia* comprising simple branching morphology with extruding corallite formation, and *P. cylindrica* having complex morphology with neutral corallite formations. Scale bar = 1 cm.

were imported into Adobe Photoshop CS3 (Adobe Systems), converted from color to 256 shades of gray and analyzed using the histogram function. The gray scale was set with black as 0 and white as 256, with any pixel receiving light energy sufficient to dilute triangulation accuracy of an active scanner being recorded as 26–256 shades of gray. These counts were normalized against the calibration target pixel size and expressed as a spot scattering index, representing the surface area reflecting light energy relevant to the source surface area on the blackened calibration tile.

Skeletal albedo—Skeletal albedo was measured using a factory-calibrated USB2000 Ocean Optics UV/Vis spectrometer coupled with a 200 µm UV-Vis optic fiber. Skeletons were illuminated with natural light under a clear midday sky (Brisbane, Australia; 27°30′, 152°00′) with a solar zenith angle of 10°. Measurements of solar irradiance were used to standardize the reflected light field from the coral with measurements being collected at 10° from vertical, 180° horizontally of the direction of the sun. This was performed to assess the spectral quantity of reflected light, from a horizontal surface of the skeletons as described in Enriquez et al. (2005).

Wax dipping and foil wrapping—Wax dipping was conducted using a modified wax dipping method taken from Stimson and Kinzie (1991) outlined in Holmes et al. (2008) using paraffin-dipping wax (Paraplast® Tissue Embedding Medium, Tyco Healthcare Group) at 65°C. Wax temperature was maintained by placing the beaker of wax in a water bath with the water temperature constantly checked using a Cyberscan pH 510 (Eutech Instruments) temperature probe and wax temperature measured regularly with an alcohol thermometer. Coral skeletons were maintained at 25°C ambient air temperature, 40°C cooler than the wax. Each coral skeleton was weighed prior to dipping, then dipped for 2 s before being removed from the wax, and rotated quickly in air (10 revolutions over 2 s) to promote an even coverage and to remove any excess wax. Dipped corals were then allowed to stand for 15 min before being reweighted. This process was repeated for the double dipping.

The increase in mass between the first and second dip was then converted to a surface area using (Eq. 1) taken from Holmes (2008).

$$\text{Surface area (cm}^2\text{)} = 34.32(\text{cm}^2/\text{g}) \times \text{mass (g)} \quad (1)$$

Foil wrapping of coral skeletons conducted based on the method of Marsh (1970). A known area of aluminum foil (100 cm^2) was cut from a roll of standard kitchen foil and weighed to determine the weight per unit area of the foil. The procedure was repeated three times to provide an average of 2.90 ± 0.03 mg/cm^2 (mean ±SD). Each coral skeleton was then carefully wrapped in the foil such that overlapping of foil was minimized. The weight of the foil required to cover each coral was then used to estimate the surface area of the coral skeleton. Each skeleton took approximately 20 min to wrap.

Photogrammetric reconstruction without projected optical texture: Photogrammetric reconstruction was performed with a Canon Powershot 630 digital camera calibrated at an object distance of 22.9 cm in Photomodeler Pro 4.0 (Eos Systems). The coral was placed on a mechanical grade turntable against a blackened background and photographed at 45° cardinal increments, 30° from the horizon. Twelve photographs were initially trialed for the processing of each coral skeleton. Not withstanding this, it was discovered that due to the lack of suitable naturally occurring reference marks on the *G. tenuidens* skeleton, the use of all 12 photographs significantly increased the root mean square (RMS) error of the surface generation. This increase in error appeared to be the result of attempting to fit too many photographs with a high degree of overlap, where point alignment in all photographs was not the same due to optical lens distortions of the camera. As only coarse morphology information could be gathered with this technique, 8 photographs were used for the *G. tenuidens* reconstruction and 10 for both the *A. intermedia* and *P. cylindrica* skeletons. In Photomodeler 4.0, each of the photographs was spatially referenced to each other using manual point digitization of all discernable features as outlined in Bythell et al. (2001). Due to the structural complexity of the *A. intermedia* and *P. cylindrical*, it was not possible to process these skeletons with this technique, with occlusions and lack of unambiguous natural targets severely limiting the capacity to identify conjugate image points. Photographic capture and spatial referencing took approximately 1 h, with the point digitization taking 3 h for the *G. tenuidens*. Point auditing was conducted in Photomodeler, removing all points with tightness values (a value used to indicate the accuracy of an object point's photo marking) > 5%. Polygons were then fitted to the network of points in Photomodeler to produce a closed surface, which was exported as Virtual Reality Modeling Language (.wrl) file into Polyworks 10 modeler node (Innovmetric Software) for final processing.

Photogrammetric reconstruction with projected optical texture—Photogrammetric reconstruction was also performed using a VX Technologies Star Cam (VX Technologies Inc) scanner that employs two CCD imaging cameras that automatically image matched an optical texture that was projected onto the coral using the instrument's integrated LCD data projector. Coral skeletons were placed 0.5 m from the scanner, in the center of a mechanical rotating stage, held in place by magnetic clamps that acted as spatial reference markers. Each scan needed to contain at least 60% of data from the previous scan to facilitate data alignment; therefore the stage was rotated by 30° per scan with a total scanning time of approximately 1 h per skeleton. Coral scans were exported from the ShapeCapture SC (VX Technologies) data acquisition program as Polyworks Interface (.pol) files for further processing in Polyworks 10, Align node (Innovmetric Software), where scans were registered using a three-point referencing system and automatically reconstructed into a 3-D shape. Shapes were then automatically cleaned, with any gaps in the surface that were less than 10 points in circumference-filled and with any free-standing closed shapes with 20 sides or less that were not in direct contact with the primary surface were removed. The resulting cleaned file was exported as a single surface .wrl file for further processing in Polyworks 10, Modeller node.

Structured light reconstruction using a projected laser (laser scanning)—Laser scanning was conducted with a Polhemus Fastscan Scorpion handheld laser scanner, as outlined in Holmes (2008). This is a structured light solution, comprising a metric scanner that projects a 1-mW red laser fan across the surface of the object and two CCD cameras that each image the resultant cross-sectional profile. The solution for three-dimensional position is based on triangulation of the projected laser and the imaged profile. The "Scorpion" version of the hardware has two imaging cameras, which reduces the chances of a point on the object being missed because of occlusions. A reference signal transmitter is placed close to the object, enabling spatial referencing (position and orientation) of the wand as it is moved. The raw scan data file was processed using the Fastscan software (Polhemus), smoothing the scanned surface to a resolution of 2000 µm to remove duplicate vertices. This data file was then exported as a .wrl file to Polyworks for additional manual postprocessing.

X-ray CT scanning—X-ray CT scanning was performed on a Toshiba Asteion TSX-021A multi slice, 4 times helical scanner. Each coral skeleton was placed inside the scanner on the slide table and processed using the Toshiba X-ray CT presetting for cervical spine, base emission setting of 120 kv at 135 mA. Each skeleton was scanned with an isotropic resolution of 0.5 mm × 0.5 mm × 0.5 mm, with a slice size of 512 × 512 pixels. Scans were stored as Digital Imaging and Communication in Medicine (DICOM) files (.dcm). Samples were postprocessed in Amira 5.0 (Visage Imaging) by importing the .dcm files, then using the Isosurface creation tool to build a surface based on the most rapid density change at the air-skeleton interface as outlined in Laforsch et al. (2008). Threshold setting was achieved by first visually inspecting the coral skeleton and manipulating the threshold function to produce the most

realistic operator perceived reconstruction. Three-dimensional distance measurements using the 3D Ruler tool were then collected from 10 points on each modeled coral skeleton reconstruction and were compared with measurements collected from the real skeleton using digital calipers (Mitutoyo), accurate to 0.01 mm. Differences of less than 0.1 mm were observed between all measured points, confirming the accuracy of the operator's visual threshold analysis. In all cases, this threshold value was set at –500, slightly higher than –354, used in Naumann et al. (2009). Samples were then visually inspected before being exported as a .wrl file for further post processing in Polywork 10, Modeller node.

Polyworks processing—Postprocessing using Polyworks 10 involved the following steps: (1) Multi-image photogrammetry (Photomodeler) output data were first checked for appropriate scaling and surface generation using the ruler tool, before being aligned and cropped to a plane for inter-comparison; (2) Projected optical texture scanner (StarCam) output data were processed as per the Photomodeler data to determine accurate spatial referencing. The surfaces required some minor hole filling and erroneous polygon removal from blind spots in the scan or overlapping scans resulting in surface artifacts. These were cleaned and filled before being cropped for the final comparisons. (3) Laser-scanning data were processed in the same way as the previous two photogrammetric data sets, however there were some small surface anomalies where polygons were inversely coded, requiring cleaning and reconstruction prior to cropping; (4) X-ray CT scanner files from the Amira 5.0 Isosurface function were already cleaned, however several internal polygon formations, caused by air deep inside the skeleton's corallites, needed to be removed from the inside of the structure prior to final surface cropping. The final comparison was conducted by loading all the surface models from each method into one file so they could be aligned with an appropriate offset, then trimming, prior to surface area calculations. This ensured that all corals were cropped on the same plane so that differences in surface area were directly related to surface resolution. The surface area tool was then used to extract the final surface areas of each 3-D model reconstruction.

Assessment

Scattering of projected light—In all coral skeletons, light from the LCD projector was subject to less scattering that light from the 1-mW laser source (Fig. 2). The *G. tenuidens* skeleton (GS) was the most susceptible to internal light scattering, due to its complex corallite structure. *P. cylindrica* (PS) and *A. intermedia* (AS) skeletons both had similar level of internal scattering, however if the *A. intermedia* skeleton was treated with a matte white paint (AW), the internal scattering reduced by > 35%. The *A. intermedia* skeleton that was spray painted matte black (AB) had the lowest scattering values from both laser and LCD-projected light. Yet, it was later found that this treatment absorbed excessive amounts of the emitted signal, making active projection shape capture impossible due to insufficient

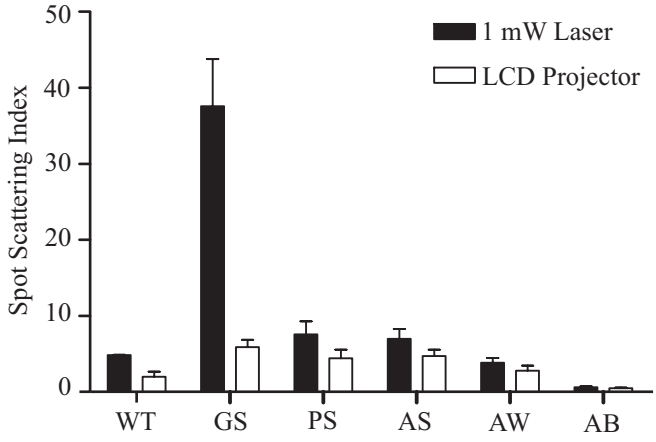

Fig. 2. Graph of coral skeletal scattering from 2 emission sources: 1-mW red laser (black) and LCD projector (white) with standard error bars. Scattering surfaces (L-R): white matte spray-painted tile (WT), *Goniopora tenuidens* skeleton (GS), *Porites cylindrica* skeleton (PS), *Acropora intermedia* skeleton (AS), white matte spray-painted *A. intermedia* skeleton (AW), and black matte spray-painted *A. intermedia* skeleton (AB). Spot-scattering index represents the surface area of the scattered light, expressed as a function of the surface area of the emission source projected onto a painted matte black calibration tile.

reflected signal strength for detection by both scanners. The results from Fig. 2 are visually displayed in Fig. 3, depicting the optical transparency of the 1-mW laser (a–d) and projected LCD light (e–h) on a matte black calibration tile (a and e), *G. tenuidens* skeleton (b and f), *P. cylindrica* skeleton (c and g) and *A. intermedia* skeleton (d and h). The internal scattering and backlighting from the *G. tenuidens* skeleton (Fig. 3b) significantly degraded triangulation accuracy for the active projection systems. The albedo of the coral skeletons (Fig. 4) revealed that all corals had high reflectance of visible light from 450 to 630 nm, with strong skeletal absorption outside these wavelengths. The *A. intermedia* skeleton that was spray painted matte black reflected less than 10% of the solar irradiance. The overall scattering was greatest from the 1-mW red laser. However, it is important to note that the 1-mW intensity of the red laser (representing the output intensity of the laser scanning wand used in this experiment), was a significantly more powerful emission source than the LCD projector used in the projected optical texture application.

Comparison of surface area and three dimensional shape representations—The comparison of surface area extraction of coral skeletons is presented in Table 2. The isotropic 500-µm X-ray CT method was deemed to be the method with the highest accuracy and resolution for determining surface area. Therefore, it was decided that all other methods would be assessed against it for accuracy, as recommended by Laforsch et al. (2008). The *G. tenuidens* skeleton was the hardest skeleton from which to extract meso-architectural surface area, due to the deep internal corallite formation, with all methods underestimating the surface area by 30% when compared with X-ray

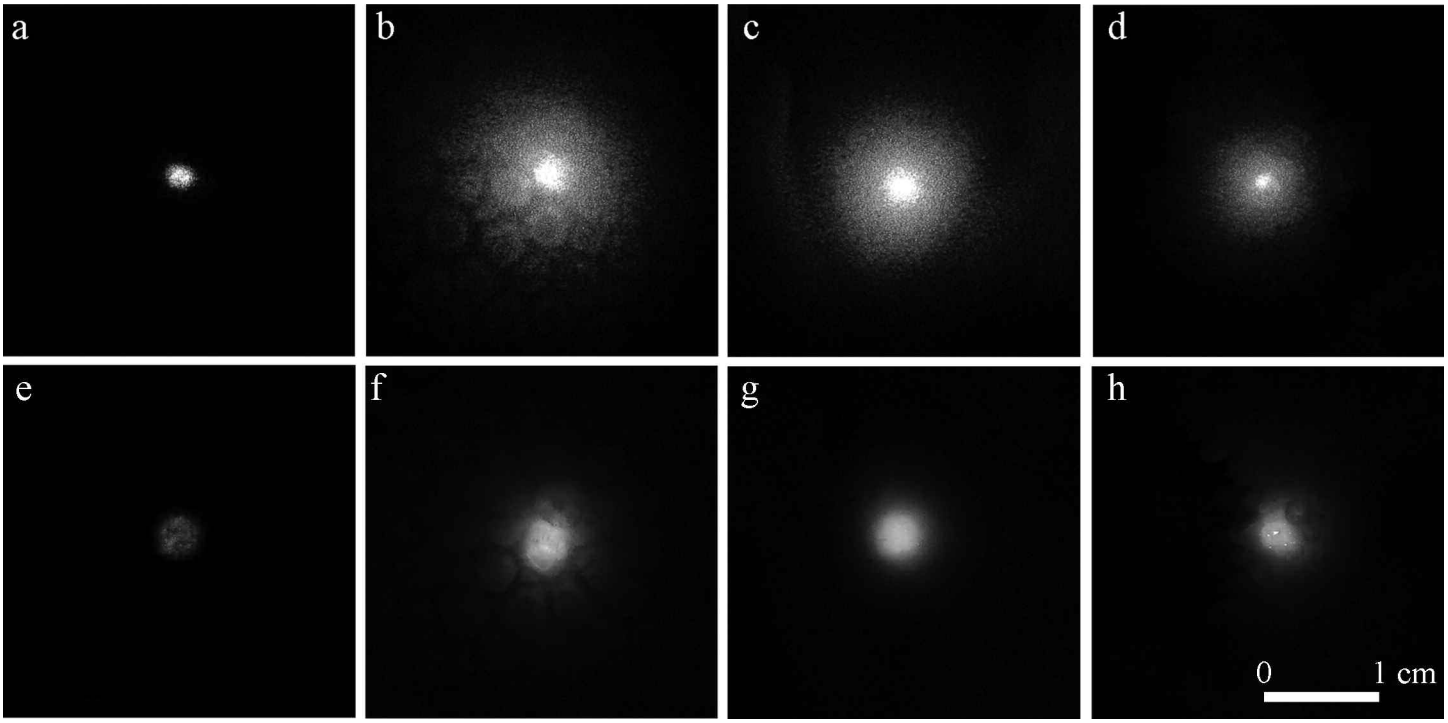

Fig. 3. Composite figure of 1-mW red laser scatter from different skeletal surfaces and treatments: (a) spray-painted matte black limestone tile, (b) untreated *Goniopora tenuidens* skeleton, (c) untreated *Porites cylindrica* skeleton, (d) untreated *Acropora intermedia* skeleton. Contrasted against structured light scatter from different skeletal surfaces and treatments: (e) spray-painted matte black limestone tile, (f) untreated *G. tenuidens* skeleton, (g) untreated *P. cylindrica* skeleton, (h) untreated A. *intermedia*. Scale bar = 1 cm.

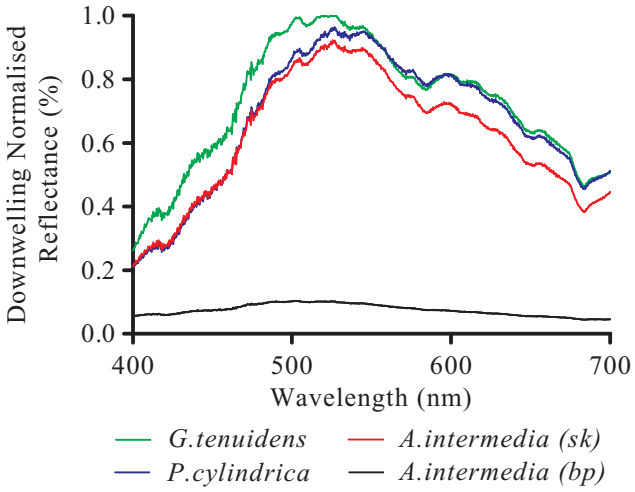

Fig. 4. Coral skeletal albedo of *Goniopora tenuidens*, *Porites cylindrica*, *Acropora intermedia*, and spray-painted matte black *A. intermedia* skeletons, illuminated in the visible spectrum (400 to 700 nm) by midday sun in Brisbane, Australia (27°30′, 152°00′) at 10º from solar zenith, normalized as a function of incoming irradiance.

CT. The 3-D surface reconstructions, from which the surface area measurements were collected, for the *G. tenuidens* skeleton are displayed in Fig. 5 with (a) photogrammetric reconstruction using ambient light and the Photomodeler software, (b) the FASTScan laser scanner, (c) photogrammetric reconstruction using projected light and the StarCam scanner, and (d) X-ray CT reconstruction. The photogrammetric reconstruction without projected light clearly highlights the limitation of this method, with manual point identification resulting in an overly simplistic surface, especially on the dorsal surfaces, where limited point identification was possible. Results for the photogrammetry that uses projected light scanning show that some of the meso-architecture has been detected. However the method of surface reconstruction results in overlapping data at the edge of each scan, reducing the accuracy of corallite detection. Laser scanning was only capable of detecting the gross morphological structure of the skeleton, however it was the second fastest and easiest method to acquire and process spatial data. X-ray CT scanning accurately depicted both the gross morphological and meso-architecture of the skeleton.

The skeleton of *A. intermedia* represented a simple branching morphology with external meso-architectural surface rugosity. The wax dipping method was highly accurate with respect to the skeleton of this species, clearly detecting both the gross morphology and meso-architectural features of the coral, based on its tight agreement with X-ray CT surface area measurement. Foil wrapping overestimated the surface by 37% (Table 3), most likely caused by overlapping of the foil on the skeletal branches. A comparison of 3-D surface reconstruc-

Table 3. Surface areas measurement from *Goniopora tenuidens*, *Porites cylindrical*, and *Acropora intermedia* skeletons using X-Ray CT, structured light scanning, laser scanning, photogrammetric reconstruction, wax dipping, and foil wrapping. These were then expressed as a function of most accurate method tested, X-ray CT surface area, to determine levels of accuracy of each methods surface area calculation.

	G. tenuidens	*A. intermedia*	*P. cylindrica*	*G. tenuidens*	*A. intermedia*	*P. cylindrica*
Units	cm^2	cm^2	cm^2	% X-ray CT	% X-ray CT	% X-ray CT
X-ray CT	203.30	86.03	205.84	100.00%	100.00%	100.00%
Structured	142.91	82.73	186.33	70.30%	96.16%	90.52%
Laser	136.62	73.69	191.55	67.20%	85.66%	93.06%
Photo	133.80	N/A	N/A	65.81%	N/A	N/A
Wax	139.69	85.33	200.36	68.71%	99.19%	97.34%
Foil	134.00	137.16	216.00	65.91%	137.16%	104.93%

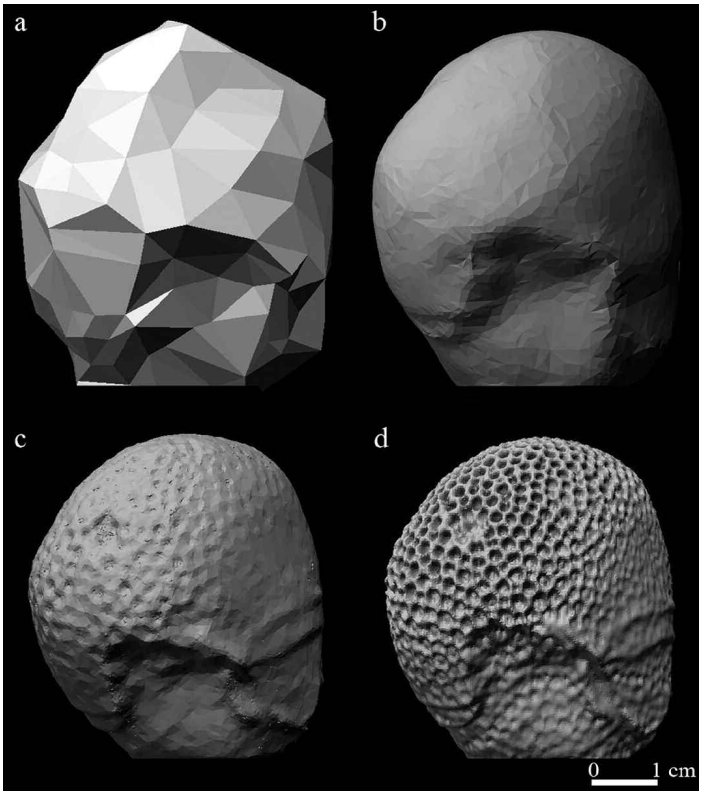

Fig. 5. Composite figureof 3-D reconstruction of the *Goniopora tenuidens* skeleton from (a) photogrammetric, (b) laser scanning, (c) structured light scanning, and (d) X-Ray CT reconstructions.

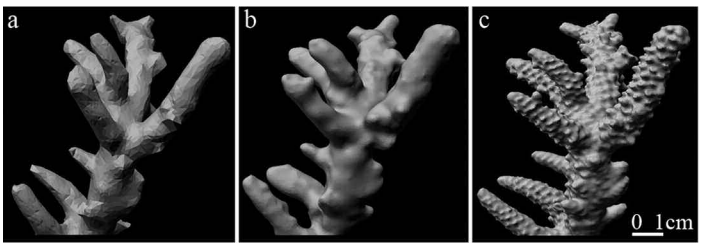

Fig. 6. Composite figure of 3-D reconstruction of the *Acropora intermedia* skeleton from (a) laser scanning, (b) structured light scanning, and (c) X-Ray CT scanner.

tion (Fig. 6) reveals that the laser scanner (a) appeared to detect the base of the coral branch, missing the extruding corallite structure, resulting in reduced branch thickness. The projected light solution (b) inversely detected the surface at the top of each corallite, filling in the gaps between corallite tips to create a smooth surface, overestimating branch width. Despite this overestimation of branch thickness, failure to detect external corallite surface area (the surface area on the sides of each corallite) resulted in a net underestimation of surface area, compared to the X-ray CT measurements. The X-ray CT (c) again accurately depicted the gross morphology and corallite formation of the *A. intermedia* skeleton. The *P. cylindrica* represented the most complex morphology scanned; however it only had gross morphological features, with the corallites too small to be detected with any of the methods outlined in this paper. The biggest challenge with this morphology was the self shading by the complex branching structures, making optical scanning challenging. Wax dipping again best estimated the surface area, closest to that calculated from X-ray CT scanning, followed by laser scanning then optical texture scanner. Laser scanning presented significant advantages with this type of complex morphology, as the operator was able to scan regions multiple times, and check in real time that the complex morphological architecture of the colony was properly detected, a technique not possible when using the projected light system.

Discussion

The calculation of biotic surface area is a key to understanding an organism's interaction with its surrounding environment (Edmunds and Gates 2002). Furthermore, the morphological complexity of Scleractinian coral reefs and their interaction with the aquatic medium cannot be fully explained without reference to their surface area (Dahl 1973). This study compared six methods for capturing surface area and shape information from coral skeletons, finding some methods to be clearly wanting when compared with the X-ray CT scanning standards, which is the most accurate method currently available for use on coral skeleton (Laforsch et al. 2008; Naumann et al. 2009). The three coral skeletons selected

for this research were designed to represent a wide range of commonly exhibited gross morphological and meso-architectural characteristic.

The use of active scanners for 3-D surface area and shape capture has become increasingly popular over the last 10 years due to reduced costs and increasing computational power, facilitating easier scanning of complex high resolution objects (Remondino and El-Hakim 2006). The optical properties of the object being scanned are integrally linked to the success and accuracy of the scanning (Beraldin et al. 2005). The reflectance of visible irradiance (400 to 750 nm) from a bleached coral skeleton displayed a spectral shift, with light at 750 nm being completely reflected, reducing exponentially to only 65% reflected at 400 nm (Stambler and Dubinsky 2005). Non-Lambertian properties of coral skeletons are also significantly influenced by ambient lighting environments that provide contrast to the images, making feature identification easier (Voisin et al. 2007). The downside to ambient lighting is that it dilutes projected emission on the surface, degrading the accuracy of point triangulation (Voisin et al. 2007). Triangulation error using an LCD emission source, projected onto the White 9.5 reference tile of the MacBeth ColorChecker chart (GretagMacbeth), which closest represents coral skeleton color, revealed 20 times greater error under external ambient light and 15 times greater under indoor fluorescent lights compared with optimal dark room conditions (Voisin et al. 2007). The influence of color and lighting is therefore important to the success of optical scanning of corals, however optical transparency of the surface is the greatest limitation to the overall resolution of the shape capture.

The optical properties of coral skeletons are integrally linked to both the calcium carbonate building materials and the skeletal meso-architecture (Barnes and Devereux 1988). Scleractinian coral skeletons grow through a process of progressive secretion of aragonite ($CaCO_3$), forming deposits in needle-shaped, acicular crystals, approximately 1 µm wide and up to 10 µm long (Buddemeier et al. 1974). The packing of the crystal and, subsequently, the overall density of the coral affects the homogeneity of surface albedo and optical transparency at the coral micro-architecture scale (Barnes and Devereux 1988). Studies investigating the optical properties of the micro-architecture of marble (metamorphosed $CaCO_3$) revealed that marble departed from an "ideal surface" due to variable crystal alignment and density fluctuations, making it translucent and optically nonhomogenous (Godin et al. 2001). Coral skeletal density also varies significantly between species and with fluctuations in abiotic variables, with the greatest amount of variability controlled by the corallite structure, which dictates skeletal internal scattering and albedo properties (Barnes and Devereux 1988; Stolarski, 2003). Skeletal scattering was first highlighted in detail by Enriquez et al. (2005), observing that light would scatter multiple times within the coral skeleton and thereby increase the chance of light absorption by symbionts. This high potential of the coral skeleton to scatter light is reflected in the results with significant scattering of both projected white light signals and more significantly laser light, leading to reduced accuracy of surface detection.

Wax dipping to measure surface area of coral skeletons has formed the basis of numerous coral research experiments (Stimson and Kinzie 1991; Chancerelle 2000; Holmes et al. 2008). The current method of double wax dipping results in a reduction in the ability to detect internal coral meso-architecture yet was still able to detect extruding corallite formations, supported by Naumann et al. (2009). Holmes (2008) observed that wax dipping had an approximate spatial resolution of 2000 µm^2 when compared with a laser scanner; however results from this study suggest that on smooth, externally rugose corals, the resolution may be finer. Wax dipping had the highest accuracy for surface area extraction methods, compared against X-ray CT, for both the *P. cylindrica* and *A. intermedia* skeletons, and second highest in the *G. tenuidens* (Table 3). Wax dipping, although destructive, is the fastest and most cost-effective method to extract surface area data from large numbers of coral skeletons with varying morphology, especially in remote locations.

The use of foil wrapping to estimate surface area is one of the oldest documented methods of coral surface area extraction and has been extensively used in studies to date. Compared with other methods of surface area detection, foil appears to overestimate the surface area, with multiple authors noting surface area over predictions of 13% to 20% when compared to dye dipping (Hoegh-Guldberg 1988), photogrammetric reconstruction (Bythell et al. 2001), and stereo video (Cocito et al. 2003). This research supports these statements with both the branching morphologies, especially the *A. intermedia* being overestimated. The complex morphology of the *P. cylindrica* was the most time consuming and challenging skeleton to measure with this method, with the authors suggesting that complexity or size of samples greater than those used in this study would be near impossible to measure with adequate accuracy using this technique. The largest source of error appears to come from foil overlapping on the edges (Hoegh-Guldberg 1988; Bythell et al. 2001).

Photogrammetry still remains the most portable, cost-effective, and flexible method for nondestructive shape capture (Niem et al. 1999). Developments in 3-D photogrammetric reconstruction software enabled Bythell et al. (2001) to reconstruct the surface area and shape of massive morphology corals for the first time. Courtney et al. (2007) extended this technique to more complex branching morphologies of *Acropora palmata*, however the large branch size and lack of branch surface occlusion made photographic reconstruction easier than the complex 100-mm-thick branches of *A. intermedia* used in this study. Notwithstanding the advantages of photogrammetry, the ability to work on complex, nonhemispherical corals is still not proven, primarily hampered by complex occlusions, the high degree of user interactivity, long process-

ing times, and problems with model alignment on complex skeletons (Bythell et al. 2001).

Reconstruction of in situ massive and submassive coral morphologies from stereo video using custom built software has also been successfully tested on Mediterranean corals. This method was limited by the 4-h long processing time and use of a large reference frame, which had to be visible in all of the video frames, restricting its application to small scale projects (Bythell et al. 2001; Cocito et al. 2003). Simple photogrammetric reconstruction of coral nubbins used in scientific experiments, obtained by tracing a series of circular splines onto aligned photograph has proven to be a quick, effective, and nondestructive way of estimating surface area of live coral fragments, achieving the same resolution as wax dipping (Jones et al. 2008).

Results from this study encountered similar limitation previously documented by other authors (e.g., Bythell et al. 2001). Large processing time and a lack of accurate surface area detection on complex 3-D forms limited this photographic method's further application to coral skeleton surface area detection, within the current software constraints. Further to this, the *G. tenuidens* skeleton was devoid of easily identifiable surface features, in contrast to corals with live tissue that were used in Bythell et al. (2001). This made accurate point identification, especially on the dorsal surface of the skeleton inadequate, resulting in lower quality surface area reconstructions.

Previous investigations of photogrammetry for coral mapping have employed software that required the user to observe and digitize each measured image point discretely in each of two or more images. An alternative approach is to extract three-dimensional coordinates using automatic image-matching algorithms. For example, image patches comprising 15 by 15 pixels in each of two or more photographs can be automatically compared using an image-matching algorithm that computes an image correlation coefficient between an image template in one image and a moving window in another image (Wolf and DeWitt 2000). Corresponding (conjugate) points in two or more images are thus automatically identified, and their three-dimensional coordinates computed using standard photogrammetric methods. This approach allows an object's surface to be mapped at very high resolution. The application of this method to the mapping of corals has not been previously reported and, while it does not address the problem of occlusions in complex morphologies, might be expected to improve the resolution of the surface matching. Work undertaken by Grenness et al. (2008) indicates the potential of close-range stereo photogrammetric mapping of biological surfaces.

Laser scanning, although occasionally used on corals (Holmes 2008; Raz-Bahat et al. 2009), is used extensively in cultural heritage digitization as a high resolution, fast, noncontact method of scanning objects (Beraldin et al. 2002; Godin et al. 2002) with 50 μm^2 resolution possible under ideal conditions and surface properties (Hahn et al. 2007). Holmes (2008) found this to be much closer to 2000 μm^2 when scanning optically transparent coral skeletons, finding that wax dipping and laser scanning produced similar surface area calculations. However all corallite meso-architecture smaller than 2000 μm^2 was discarded. This is clearly evident in this study with the *A. intermedia* skeleton, where the surface reconstruction occurred at the base of the corallite polyps, generating thinner branches than the actual skeleton (Fig. 6). This phenomenon can partly be attributed to the optical properties of the surface as previously outlined, with surface identification subject to speckled noise and multiple surface reflections deep in grooves of the surface (Hahn et al. 2007). The reconstruction of the *P. cylindrica* skeleton illustrated the advantage of interactive user scanning, with the laser beam and wand configuration better able to collect spatial information from deep inside the shadowed complex morphology, compared with the more stationary projected optical texture method. This method was the second fastest of the noncontact methods with sample data collection taking 1 h and processing taking less than 2 h.

Projected optical texture scanners under ideal conditions can reach pixel resolution of 300 µm, however with the effects of ambient lighting and surface properties of corals, 1000 µm is more realistic (Voisin et al. 2007): a conclusion support by this research. The intensity and spectral properties of the white light projection system resulted in significantly less scattering on the coral skeleton surface, compared with laser systems, while still being able to produce high resolution information on intruding and extruding surface meso-architecture. Although yet to be fully developed, projected optical texture scanners have the potential to be used to scan live corals with more complex morphologies than other currently available optical techniques (Veal unpubl. data). Optical texture scanners have been operated inside remotely operated vehicles for underwater surveying fouling of growth of oil rig pipelines (Shape Capture pers. comm.), although in situ operation on coral reefs may still be some time away. A recent study has shown that X-ray CT can also be used to scan live corals inside a tank of sea water at higher resolutions than currently possible with projected optical texture scanning (Laforsch et al. 2008). Unlike X-ray CT, where the coral samples can be scanned alive and inside an aquarium filled with sea water (Laforsch et al. 2008), optical texture scanning and laser scanning both required approximately 1 h to scan a live coral fragment in air (Raz-Bahat et al. 2009), which will be significantly detrimental to the coral's health. The placement of the coral samples inside a small aquaria makes scanning difficult, as the signal passes through multiple mediums of varying refractive indexes, with very complex calibration required to facilitate point triangulation. In addition, the strong absorption properties of living coral tissue, due to the endolithic phototrophs absorbing high proportions of emitted signal in the visible range of the spectrum, result in poor signal strength for triangulation of points. Whether operated in air or

water, the biggest limitations in most of these systems is the processing time per sample.

The use of X-ray techniques on coral began in the 1970s to examine coral density with the use of microdensitometry of radiographs (Buddemeier et al. 1974; Chalker et al. 1985). This research, which was later expanded to investigate banding relationships, involved the thin sectioning of skeletons so that they could be X-rayed with traditional 2-D imaging techniques, and then rebuilt manually (Le Tissier et al. 1994). Many research facilities cannot afford their own scanner, instead processing their coral skeletons in medical units that produce scans with a range of slice thicknesses between 300 to 2500 µm (Kaandorp et al. 2005; Kruszynski et al. 2007). Some researchers have used micro X-ray CT scanners, which can generate slice thicknesses of just 100 µm; however sample size is very small, resulting in working with only a subset of the original coral colony (Helmie et al. 2000). What X-ray CT lacks in mobility it makes up for in resolution, with both surface and internal density information being collected, i.e., data collection not possible with other optical-scanning techniques. The surface does not have to be treated or illuminated in any special way, and complex structures that would be spatially occluded with other methods can easily be captured (Bosscher 1993). The most sizable collection of publications on this topic stemmed from work first formally documented by Kaandorp and Kubler (2001), where a *Madracis mirabilis* coral colony was scanned with a medical X-ray CT to investigate growth patterns. The slice thickness was 2500 µm, which meant that the surface corallite structure was not detected (Kaandorp et al. 2003). Using isotropic 500 µm voxels in this study, the detection of large internal and external corallite surface area was possible, however corallites smaller than 500 µm, such as in the *P. cylindrical*, were not detected. The ideal systems for processing raw X-ray CT data would be fully automated, however both in the literature and this study that was not possible. Therefore, a semiautomated method reliant on a defined skill level of the operator had to be employed (Kruszynski et al. 2007). The use of semiautomated classification systems for X-ray CT–scanned coral skeletons has been documented in Laforsch et al. (2008), finding less than 1.35% variability in surface area reconstructions, based on multiple operators processing of the same coral scan using the Amira 5.0 processing software. This minor variability supports the use of a single reconstruction of each coral surface from X-ray CT data used in this study. Previous authors have commented that the total time taken to scan and process a sample with a skilled operator is approximately 1.5-2 h, a statement supported by this study and significantly quicker than other computer-based methods detailed in this paper (Kruszynski et al. 2007).

Comments and recommendations

One surprising finding of this research that merits further examination is that the simple and inexpensive method of dipping corals in wax delivers quite accurate information about the surface area of flat or externally rugose coral skeletons. This method provides resolution of better than 2 mm^2, and more sophisticated methodologies are only needed if resolution below 2 mm^2 is required or a digital reconstruction of the surface is desired. The continuing development of automated point-matching software for photogrammetric applications is predicted in the following years to enable a higher accuracy surface area extraction to be undertaken on living coral tissue; however the price of the software and their application on structural complexity of branching corals are currently a limiting factor. The estimation of primary surface area now needs to be explored using newly emerging medical imaging techniques to determine the accurate surface area measurement of living noncalcareous and fleshing coral tissues and other flaccid algae to greater understand their biological interactions with the environment.

References

Atkinson, K. B. 1996. Close range photogrammetry and machine vision. Whittles Publishing.

Barnes, D., and M. J. Devereux. 1988. Variations in skeletal architecture associated with density banding in the hard corals, *Porites*. J. Exp. Mar. Biol. Ecol. 121:37-54 [doi:10.1016/0022-0981(88)90022-6].

Ben-Zion, M., Y. Achituv, N. Stambler, and Z. Dubinsky. 1991. A photographic, computerised method for measurements of surface area in *Millepora*. Symbiosis 10:115-121.

Beraldin, J. A. 2004. Integration of laser scanning and close-range photogrammetry – the last decade and beyond. IAPRSSIS 35(B7):972-983.

Beraldin, J.-A., M. Picard, S. F. El-Hakim, G. Godin, C. Latouche, V. Valzona, and A. Bandiera. 2002. Exploring a byzantine crypt through a high resolution texture mapped 3D model: Combining range data and photogrammetry. *In* Proceedings of the International Workshop on Scanning for Cultural Heritage Recording - complimenting or replacing photogrammetry; 2002 Sep 1–2; Corfu, Greece. National Research Council Canada (NRC-CNRC).

———, and others. 2005. Virtual reconstruction of heritage sites: opportunities and challenges created by 3D technologies. *In* Proceedings of the International Workshop on Recording, Modeling and Visualization of Cultural Heritage; 2005 May 22–27; Ascona, Switzerland. NRC-CNRC.

Bosscher, H. 1993. Computerised tomography and skeletal density of coral skeletons. Coral Reefs 12:97-103 [doi:10.1007/BF00302109].

Buddemeier, R. W., J. E. Maragos, and D. W. Knutson. 1974. Radiographic studies of reef coral exoskeletons: rates and patterns of coral growth. J. Exp. Mar. Biol. Ecol. 14:179-200 [doi:10.1016/0022-0981(74)90024-0].

Bythell, J. C., P. Pan, and J. Lee. 2001. Three-dimensional morphometric measurements of reef corals using underwater photogrammetry techniques. Coral Reefs 20:193-199 [doi:10.1007/s003380100157].

Chalker, B., D. Barnes, and P. Isdale. 1985. Calibration of x-ray densiometer for the measurements of coral skeletal density. Coral Reefs 4:95-100 [doi:10.1007/BF00300867].

Chancerelle, Y. 2000. Méthodes d'estimation des surfaces développées de coraux scléractiniaires à l'échelle d'une colonie ou d'un peoplement. Oceanol. Acta. 23:211-219 [doi:10.1016/S0399-1784(00)00125-0].

Cocito, S., S. Sgorbini, A. Peirano, and M. Valle. 2003. 3-D reconstruction of biological objects using underwater video technique and image processing. J. Exp. Mar. Biol. Ecol. 297:57-70 [doi:10.1016/S0022-0981(03)00369-1].

Courtney, L. A., W. S. Fisher, S. Raimondo, L. M. Oliver, and W. P. Davis. 2007. Estimating 3-dimensiional colony surface area of field corals. J. Exp. Mar. Biol. Ecol. 351:234-242 [doi:10.1016/j.jembe.2007.06.021].

Dahl, A. L. 1973. Surface area in ecological analysis: quantification of benthic coral-reef algae. Mar. Biol. 23:239-249 [doi:10.1007/BF00389331].

Done, T. J. 1981. Photogrammetry in coral reef ecology: A technique for study of change in coral reef communities. *In* E.D. Gomez, C.E. Birkeland, R.W. Buddemeier, R.E. Johannes, J.A. Marsh, Jr., and R.T. Tsuda [eds.] The reef and man: Proceedings of the Fourth International Coral Reef Symposium, Manila, Philippines, 18-22 May 1981. V. 2. University of the Philippines, Marine Sciences Center. p. 315-320.

Edmunds, P. J., and R. D. Gates. 2002. Normalizing physiological data for scleractinian corals. Coral Reefs 21:193-197.

Enriquez, S. E., E. R. Mendez, and R. Iglesias-Prieto. 2005. Multiple scattering on coral skeletons enhances light absorption by symbiotic algae. Limnol. Oceanogr. 50:1025-1032.

Fryer, J., H. Mitchell, and J. H. Chandler. 2007. Applications of 3D measurement from images. Whittles.

Godin, G., M. Rioux, J.–A. Beraldin, M. Levoy, and L. Cornoyer, and F. Blais. 2001. An assessment of laser range measurements of marble surfaces. *In* Proceedings of 5th Conference on Optical 3D Measurement Techniques; 2001 Oct 1–4; Vienna. p. 49-56.

———, and others. 2002. Active optical 3-D imaging for heritage applications. IEEE Comput. Graph. Appl. 22:24-36.

Grenness, M. J., J. E. Osborn, and M. J. Tyas. 2008. Mapping tooth surface loss with a fixed-base stereo camera. Photogramm. Rec. 23:194-207 [doi:10.1111/j.1477-9730.2008.00479.x].

Hahn, D. V., K. C. Baldwin, and D. D. Duncan. 2007. Non-laser based scanner for three-dimensional digitization of historical artefacts. Appl. Opt. 46:2838-2850 [doi:10.1364/AO.46.002838].

Helmie, K. P., R. E. Dodge, and R. A. Ketcham. 2000. Skeletal architecture and density banding in Diploria strgosa by X-ray computer tomography. *In*: Proceedings of 9th Int. Coral Reef Symposium 1:365-371.

Helmuth, B. S. T., B. E. H. Timmerman, and K. P. Sebens. 1997. Interplay of host morphology and symbiont microhabitat in coral aggregation. Mar. Biol. 130:1-10 [doi:10.1007/s002270050219].

Hoegh-Guldberg, O. 1988. A method for determining surface area of corals. Coral Reefs 7:113-116 [doi:10.1007/BF00300970].

———. 1999. Climate change, coral bleaching and the future of the world's coral reefs. Mar. Freshw. Res. 50:839-866 [doi:10.1071/MF99078].

———, and J. Williamson. 1999. Availability of two forms of dissolved nitrogen to the coral *Pocillopora damicornis* and its symbiotic zooxanthellae. Mar. Biol. 133:561-570 [doi:10.1007/s002270050496].

Holmes, G. 2008. Estimating three-dimensional surface areas on coral reefs. J. Exp. Mar. Bio. Ecol. 365:67-73 [doi:10.1016/j.jembe.2008.07.045].

———, J. Ortiz, P. Kaniewska, and R. Johnstone. 2008. Using three-dimensional surface area to compare the growth of two *Pocillopora* coral species. Mar. Biol. 155:421-427 [doi:10.1007/s00227-008-1040-x].

Hughes, T. P., and others. 2003. Climate change, human impacts and the resilience of coral reefs. Science 301:929-933 [doi:10.1126/science.1085046].

Jones, A. M., N. E. Cantin, R. Berkelmans, B. Sinclair, and A. P. Negri. 2008. A 3-D modeling method to calculate the surface areas of coral branches. Coral Reefs 27:521-526 [doi:10.1007/s00338-008-0354-y].

Kaandorp, J. A., and J. E. Kubler. 2001. The algorithmic beauty of seaweeds, sponges, and corals. Springer.

———, E. A. Koopman, P. M. A. Sloot, R. P. M. Bak, M. J. A. Vermeij, and L. E. H. Lampmann. 2003. Simulation and analysis of flow patterns around the scleractinian coral *Madracis mirabilis*. Philos. Trans. R. Soc. Lond. B. 358:1551-1557 [doi:10.1098/rstb.2003.1339].

———, P. M. A. Sloot, R. M. H. Merks, R. P. M. Bak, M. J. A. Vermeij, and C. Maier. 2005. Morphogenesis of the branching reef coral *Madracis mirabilis*. Proc. R. Soc. B. 272:127-133 [doi:10.1098/rspb.2004.2934].

Ketcham, R. A., and W. D. Carlson. 2001. Acquisition, optimization, and interpretation of x-rays computer tomographic imagery: applications to the geoscience. Comput. Geosci. 27:381-400 [doi:10.1016/S0098-3004(00)00116-3].

Kruszynski, K. J., J. A. Kaandorp, and R. van Liere. 2007. A computational method for quantifying morphological variation in scleractinian corals. Coral Reefs 26:831-840 [doi:10.1007/s00338-007-0270-6].

Laforsch, C., E. Christoph, C. Glaser, M. Naunann, C. Wild, and W. Niggl. 2008. A precise and non-destructive method to calculate the surface area in living scleractinian corals using X-ray computed tomography and 3D modeling. Coral Reefs 27:811-820 [doi:10.1007/s00338-008-0405-4].

Le Tissier, M. D'A. A., B. Clayton, B. E. Brown, and P. S. Davis. 1994. Skeletal correlates of coral density banding and an evaluation of radiography as used in sclerochronology. Mar. Ecol. Prog. Ser. 110:29-44 [doi:10.3354/meps110029].

Lesser, M. P., C. Mazel, D. Phinney, and C. S. Yentsch. 2000.

Light absorption and utilization by colonies of the congeneric hermatypic corals *Montastraea faveolata* and *Montastraea cavernosa*. Limnol. Oceanogr. 45:76-86.

Luhmann, T., S. Robson, S. Kyle, I. Harley [eds.]. 2006. Close range photogrammetry: Principles, techniques and applications. Whittles.

Marsh, J. A. 1970. Primary productivity of reef-building calcareous red algae. Ecology 51:255-263 [doi:10.2307/1933661].

Meyers, J. L., and E. T. Schultz. 1985. Tissue condition and growth rate of coral associated with schooling fish. Limnol. Oceanogr. 30:157-166 [doi:10.4319/lo.1985.30.1.0157].

Naumann, M. S., W. Niggl, C. Laforsch, C. Glaser, and C. Wild. 2009. Coral surface area quantification-evaluation of established techniques by comparison with computer tomography. Coral Reefs 28:109-117 [doi:10.1007/s00338-008-0459-3].

Niem, W. 1999. Automatic reconstruction of 3-D objects using a mobile camera. Image Vision Comput. 17:125-134 [doi:10.1016/S0262-8856(98)00116-4].

Odum, H. T., and E. P. Odum. 1955. Tropic structure and productivity of a windward coral reef community on Eniwetok Atoll. Ecol. Monogr. 25:291-320 [doi:10.2307/1943285].

Raz-Bahat, M., H. Fibish, T. Mass, and B. Rinkevich. 2009. Three-dimensional laser scanning as an efficient tool for coral surface area measurement. Limnol. Oceanogr: Methods 7:657-663.

Remondino, F., and S. El-Hakim. 2006. Image-based 3-D modeling: a review. Photogramm. Rec. 21:269-291.

Stambler, N., and Z. Dubinsky. 2005. Corals as light collectors: an integrated sphere approach. Coral Reefs 24:1-9 [doi:10.1007/s00338-004-0452-4].

Stimson, J., and R. A. Kinzie. 1991. The temporal pattern and rate of release of zooxanthellae from the reef coral *Pocillopora damicornis* (Linnaeus) under nitrogen-enrichment and control conditions. J. Exp. Mar. Biol. Ecol. 153:63-74 [doi:10.1016/S0022-0981(05)80006-1].

Stolarski, J. 2003. Three dimensional micro- and nanostructural characteristics of scleractinian coral skeleton: a biocalcification proxy. Acta. Palaeontol. Pol. 48:497-530.

Voisin, S., S. Foufou, F. Truchetet, D. Page, and M Abidi. 2007. Study of ambient light influence for three-dimensional scanners based on structured light. Opt. Engi. 46 [doi:10.1117/12.740641].

Wöhler, C. 2009. 3D computer vision: Efficient methods and applications. Springer.

Wolf, P. R., and B. A. DeWitt. 2000. Elements of photogrammetry (with applications in GIS). McGraw-Hill Higher Education.

Yentsch, C. S., C. M. Yentsch, J. J. Cullen, B. Lapointe, D. A. Phinney, and S. W. Yentsch. 2002. Sunlight and water transparency: cornerstones in coral research. J. Exp. Mar. Biol. Ecol. 268:171-183 [doi:10.1016/S0022-0981(01)00379-3].

Submitted 22 October 2009
Revised 28 February 2010
Accepted 16 March 2010